New Thresholding Methods for Unimodal Images of Food and Agricultural Products

Sunil K. Mathanker *and* Paul R. Weckler

Abstract— **Global thresholding methods fail to segment poor contrast unimodal food and agricultural images. Many local adaptive thresholding and multi-level thresholding methods are reported in image processing journals, but there are limited studies extending them to food and agricultural images. This article presents development of Reverse Water Flow, a new local adaptive thresholding method, and Twice Otsu, a new multi-level thresholding method, to segment food and agricultural images. Reverse Water Flow method was well suited for identification of smaller objects such as 2 mm diameter holes. It reduced computational time by 61.1% compared to the previous best method. Twice Otsu method was well suited to identify larger objects. Both thresholding methods successfully segmented food and agricultural images from different imaging sources and should be extendable to other unimodal and poor contrast images. The developed methods may also facilitate further development of segmentation methods for food and agricultural applications.**

Index Terms— **agriculture, food, image processing, local adaptive thresholding, machine vision, multi-level thresholding, segmentation, thresholding, unimodal images.**

1. INTRODUCTION

Image segmentation is one of the challenging operations in many machine vision applications. The task becomes much more challenging when it comes to food and agricultural images. These images are typically poor contrast and have unimodal histograms (Fig. 1). Most global thresholding methods fail to segment them [1] because these methods typically require a bi-modal histogram. An object of interest (defect) generally shows slightly different contrast (Fig. 1b) and many times it is hard to tell whether the difference is due to a natural variability or presence of a defect. In such a scenario, local adaptive thresholding methods can play a significant role because they take local image properties in consideration which generally results in better segmentation.

The variance based Niblack method calculates image threshold value based on local mean and standard deviation [2]. In window partition methods, an image is divided into sub images based on a selected criterion: Lorentz information measure [3], equal sized image partition [4], and learned image partition rule [5]. Water flow analogy methods consider image surface as a three dimensional surface [6]. Other approaches

reported in literature are mean shift and clustering for multimodal feature space [7], gray level reduction [8], and gray level co-occurrence matrix [9]. A review and raking of thresholding methods can be found in [10].

Another approach to segment unimodal images is multi-level thresholding which segments a gray image into more than two segments. The multi-level thresholding method of Otsu [11] is probably the first and most well-known method. Thereafter, a variety of approaches have been proposed to determine multiple thresholds: mean and variance of pixel distribution [12], edge and intensity information [13], global valleys search and transformation [14], mini-max optimization [15], fuzzy and rough set theories [16], entropy [17], Gaussian distribution [18], and minimizing fuzziness [19].

To address segmentation of unimodal pecan x-ray images, Reverse Water Flow method, a local adaptive thresholding method, was proposed to segment smaller defects [1]. Similarly, Twice Otsu method, a multi-level thresholding method, was developed to segment larger pecan defects [20]. Both these methods improved pecan defect classification accuracy using computationally efficient classifier AdaBoost [21]. Both the segmentation methods can be extended to other segmentation tasks as well, and this article aims to provide detailed development of Reverse Water Flow method and Twice Otsu method.

2. DEVELOPMENT OF REVERSE WATER FLOW METHOD

Based on the reviewed studies, it was hypothesized that water flow analogy method of Oh et al. [22] could adapt well to the natural variations in shape and size of defects present in food and agricultural images. Oh method can be divided in two parts: water flow process and thresholding criterion determination. In the water flow process, water drops are poured at gradients points, and the water drops flow to regional minimum points and get deposited there. A stopping criterion is used to stop the iterative water flow process. A threshold is used to segment the amount of water deposited. Fig. 2 shows the segmentation results at various stages of Oh method for a typical pecan image. In the Oh water flow process, water drops deposited in the central portion of nutmeat halves (Fig. 2c) traveled from far

distant water drop points (gradient points) mainly on the nut halves edges (Fig. 2b). These longer travels require lot of computational time. If these travel times could be reduced then considerable time can be saved. Complex and cumbersome determination of thresholds was another limitation of Oh method. Multiple optimizations, determination of empirical constants, and recalculations to achieve better segmentation were the other limitations of Oh method. Reverse Water Flow method aimed to overcome limitations of Oh method. The development of Reverse Water Flow method is also divided into two parts.
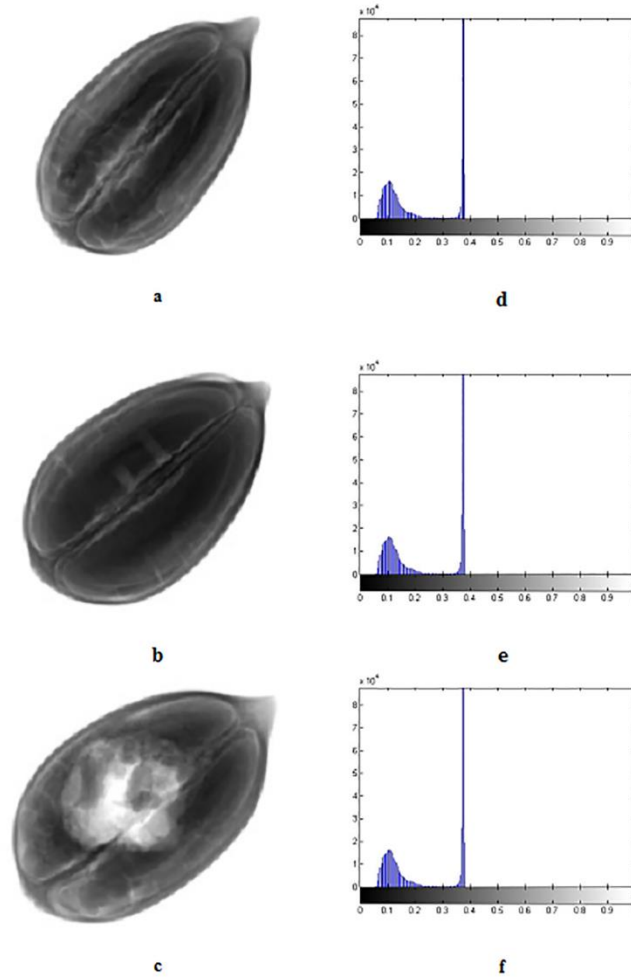

Fig. 1. Typical unimodal x-ray pecan images used in non-destructive testing: (a) good pecan, (b) pecan with small defect (2 mm diameter insect exit hole), and (c) pecan with a large defect (large portion of nutmeat eaten away by insects); (d), (e), and (f) histogram of image (a), (b), and (c).
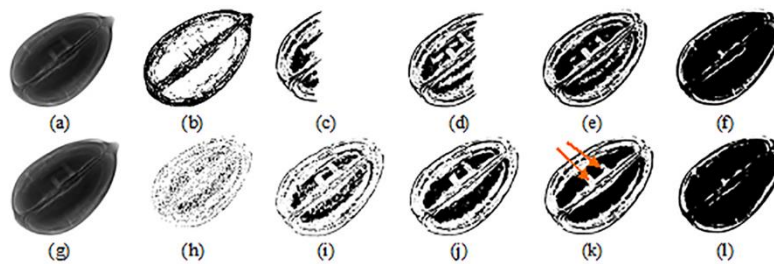

Fig. 2. Progression of water flow process for the Oh and Reverse Water Flow method: original images (a and g), gradient points (b), local minima points (h), water flow progression when 10% gradient points are submerged (c and i), 20% submerged

(d and j), 30% submerged (e and k) and 80% submerged (f and l).

2.1 Reverse Water Flow Process

In the reverse water flow process, the image to be segmented is considered as a three dimensional space (Fig. 3). A pixel area is considered as a surface location and pixel intensity as elevation of that surface. After Gaussian smoothing with unit variance, the image is searched for local minima points. A water drop is poured at a local minima point. When a water drop is poured at the local minima point, a search for a regional minimum point at that moment is initiated. A typical travel path followed by a water drop is illustrated in Fig. 4. If a water drop is poured at location 1, mask 'A' (5x5 mask) finds the minimum intensity level (elevation) around location 1. If location 2 is the location with minimum elevation in mask 'A', the water drop flows to location 2. A new mask 'B' detects the new location with minimum elevation within mask 'B'. If location 3 is the location with minimum elevation in mask 'B', the water drop flows to location 3. This process is continued until the center location of the mask is the minimum elevation within the mask. If location 3 is the minimum point at the center of mask 'C', then the search has reached the regional minimum elevation point. After completion of the search process, the water drop gets deposited at the regional minimum point. The water drop deposition raises elevations of the regional minimum point and its neighboring pixels (Fig.4).

The Oh water flow process drops water at the higher magnitude gradient points (circular red dots in Fig. 5), mostly at higher elevations (Fig. 3). The water drops poured at the gradient points have to travel longer distances (shown by red dashed arrows in Fig. 5). In contrast, the developed reverse water flow process uses local minima points (shown by blue squares in Fig. 5) as water drop points. The situation 'A' in Fig. 5 refers to the first iteration of the water flow process. The water drop poured at a local minima point gets deposited there itself and does not has to travel any distance. Once the search has reached the regional minimum point, the pixel intensity values of the neighboring pixels are increased as follows:

$$I^{'}(x_{M+j}, y_{M+k}) = I(x_{M+j}, y_{M+k}) + \alpha G(j+1, k+1) \qquad -1 \le j, k \le 1$$
(1)

Where, $I^{'}(x_M, y_M)$ represents the water filled image after $(n+1)^{th}$ water drop deposition, $I(x_M, y_M)$ represents the water filled image after $(n)^{th}$ water drop deposition, x_M, y_M represents regional minimum point, G(j, k) represents the 3x3 Gaussian mask with unit variance and α controls the amount of water filled at local minimum point and eight surrounding

pixels. Oh et al. [22] suggested $\alpha = 2$ for 8 bit images and Mathanker et al. [1] used $\alpha = 32$ for 12 bit images.

After a few iterations, the elevations of local minima points get raised due to water drop depositions. Then water drops poured at the local minima points have to travel longer distances, for example to location 'B' (Fig. 5). At this stage the travel distance for the proposed water drop points (local minima points) are approximately equal to a few Oh water drop points (gradient points), but still shorter than other Oh water drop points (top row of three red dots in Fig. 5). It is expected that the new water flow process might result in considerable computational time saving.

To compare the saving in computational time, progression of reverse water flow process was studied and is presented in lower row of Fig. 2. Compared to Oh method (upper row of Fig. 2), the water drops points in the reverse water flow process are uniformly distributed. For the first iteration the drops get deposited on the local minima points itself with no travel distance. In the next iterations, the water drops get deposited nearby with minimum travel distance (Fig. 2i). This phenomenon becomes evident, when water drop point locations in Fig. 2h and water deposition locations in Fig. 2i are compared. Thus, one of the shortcomings of the Oh water flow process i.e. longer water drop travel distance is addressed by the proposed reverse water flow process. Further, this becomes more evident when Fig. 2k and 2e are compared with their corresponding Figs. 2h and 2b.

The reduction in travel distance of the water drops was quantified by recording the processing (computational) time required. Reverse Water Flow method reduced the average computation time by 61.1% compared to Oh method [1]. The new concept of the proposed water flow process was probably the reason for savings in time. It reduced travel distance at initial stages which resulted in a faster algorithm. The savings in computational time can be of great help for on-line machine vision inspection of food products.

The iterative water flow process is terminated automatically by introducing a stopping criterion. The stopping criterion is defined as submergence of certain fraction of gradient points [22].

$$GP_t = C * GP_0$$
(2)

Where, GP_t = gradient points submerged at t^{th} iteration; GP_0 = total gradient points; C = fraction of gradient points allowed to submerge (adjusted to get desired segmentation results). The amount of water deposited at each pixel location is calculated by subtracting the water filled image from the original image. The resulting image is hereafter referred to as water image.
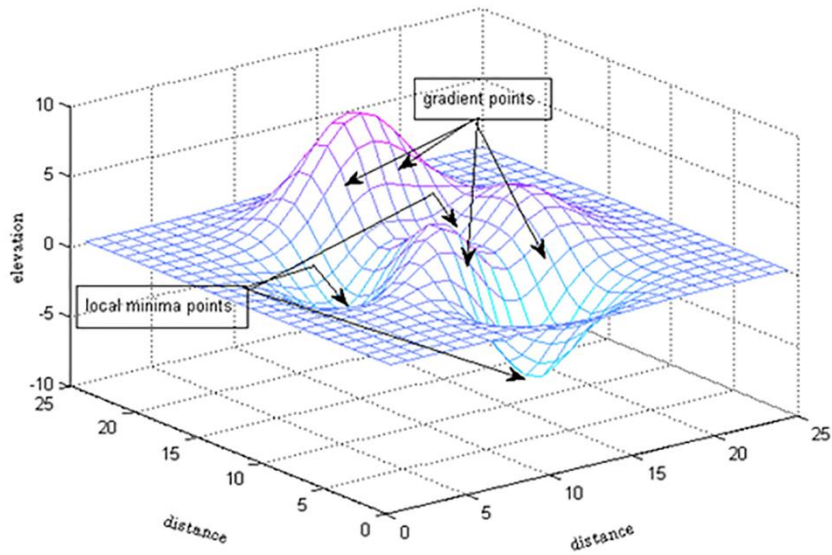
Fig. 3. Three dimensional surface with possible locations of gradient points and local minima points.
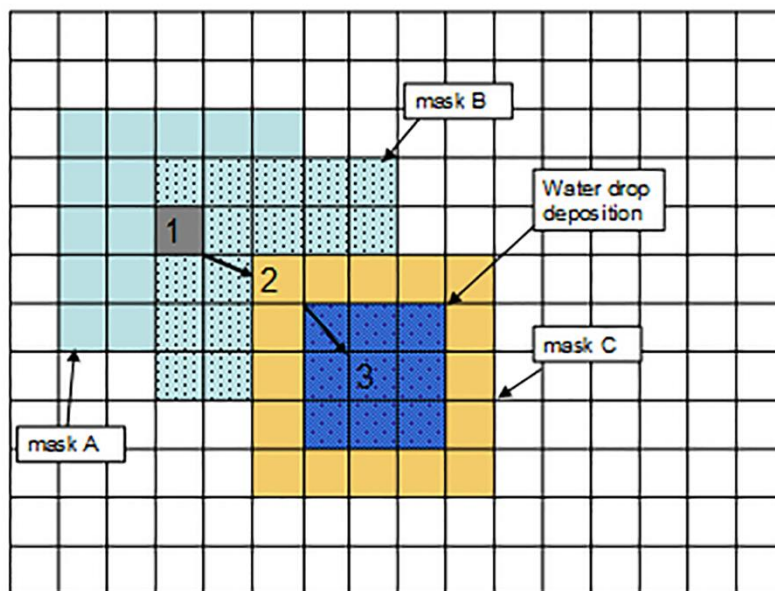

Fig. 4. Search process for regional minimum point (concept taken from Kim et al., [6]).
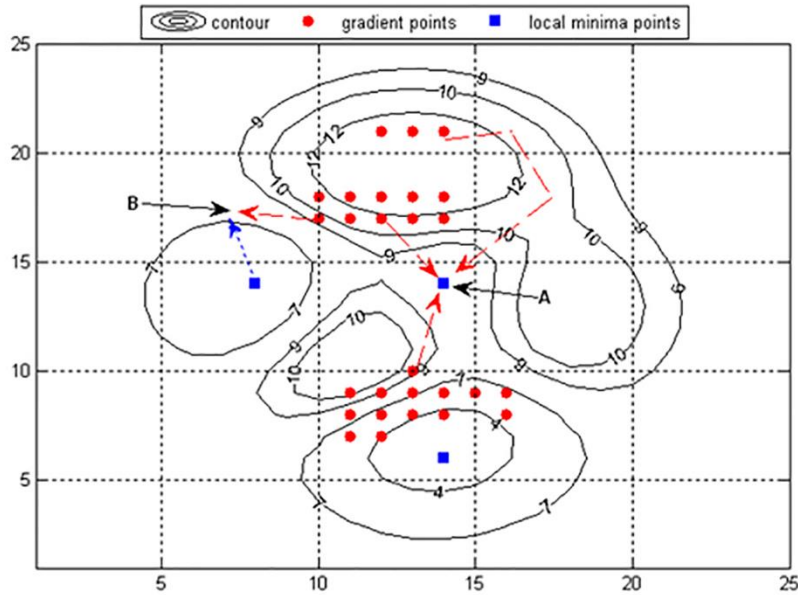
Fig. 5. Contour map of Fig. 3: illustrating possible flow paths from gradients points and local minima points (situation A: first iteration, and situation B: after a few iterations).

2.2 Local Adaptive Thresholding Criterion

The water image, obtained in previous sub-section 2.1, is segmented using a threshold. Very small water depths were considered as noise in Oh method and removed. After removing noise, Oh method [22] used two single Otsu thresholds to segment the water image. The determination of the two single Otsu thresholds involved empirical determination of separability factors three times, and adjustment of thresholds twice [22]. Further, analysis of revealed that the threshold determination is similar to Otsu [11] method of determining dual Otsu thresholds. The analysis also revealed that the dual Otsu thresholds provide a much better way to optimize thresholds, and therefore adopted in Reverse Water Flow method. The adopted threshold determination criterion adapted from [11] was:

$$n* = \sigma_B^2(k_1^*, k_2^*) = \max_{1 \le k_1 < k_1 < L} \sigma_B^2(k_1, k_2)$$

(3)

Where, η is the between class variance, k1 and k2 are the thresholds separating intensity levels L into three classes (C1 [1, …, k1], C2 [k1+1, …, k2] and C3 [k2+1, …,L]). The thresholds k*1 and k*2 maximize the between class variance η*. In the Reverse Water Flow thresholding criterion, water ponds based on pixel connectivity [22] were not delineated, and the lower level threshold was used to remove the noise. It simplified the cumbersome threshold determination process of Oh method [22]. However, to present flexibility in the noise level determination, the lower threshold can be adjusted as follows:

$$k_1^{'} = k_1^* {}^* n^* {}^* \beta$$

(4)

Where, β = threshold adjustment parameter

The image noise level is represented by the lower threshold k`1, and water depths below it are removed because they are considered as noise. Thus, the image noise level can be adjusted simply by changing the threshold adjustment parameter β. In contrast, Oh method requires recalculation of the thresholds to adjust for image noise levels. The developed method hereafter is referred to as Reverse Water Flow method.

3. DEVELOPMENT OF TWICE OTSU METHOD

Bi-level thresholding methods segment image pixels into two classes: background and object. Many images contain pixels belonging to more than two classes. To segment images with more than two classes, more thresholds are required. Otsu [11] proposed a method to determine multiple thresholds based on maximization of between class variance. However in the proposed Twice Otsu method, the single Otsu threshold method is used to divide a class in two sub-classes (Eq. 5).

$$n* = \sigma_B^2(k_1^*, k_2^*) = \max_{1 \le k_1 < k_1 < L} \sigma_B^2(k_1, k_2)$$

(5)

For example, the image in Fig. 6a is segmented into two classes: object pixels (black pixels in Fig. 6b) and background pixels (white in Fig. 6b) by applying the single Otsu threshold method. The pixels belonging to one class, say object pixels are extracted. Then, the single Otsu threshold method is applied

again to divide the extracted object pixels in two different object sub-classes. It causes some of the object pixels in Fig 6b to be classified as defective pixels (the white pixels inside pecan image, Fig. 6c). Similarly, instead of extracting the object pixels, the background pixels can be extracted and the single Otsu threshold method can be applied on them resulting in two different background sub-classes. Thus, if the single Otsu method is applied to both the object pixels and the background pixels separately then it would result in four pixel sub-classes.

This simple and intuitive process can be continued further to divide the image into any number of classes based on class variance without increasing the complexity of calculation as required in more than three class determination for Otsu method [11]. It is expected that twice application of the single Otsu method either to a) the object pixels, or b) the background pixels, or c) both type of pixels would be sufficient to segment most non-destructive images. Therefore, this method is hereafter referred to as Twice Otsu method.
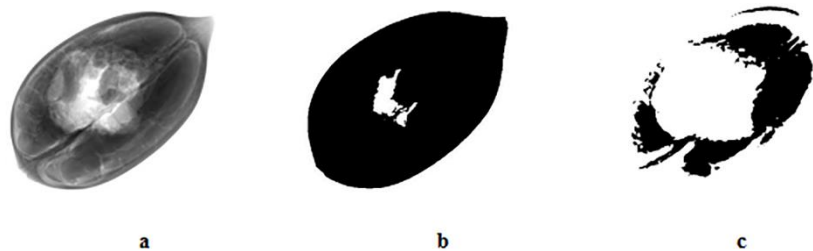

Fig. 6. Steps of Twice Otsu segmentation method: (a) Original image, (b) segmented image after first application of single Otsu threshold method on (a), (c) segmented image after second application of single Otsu segmentation on object (dark) pixels of image (b).

4. EXPERIMENTAL RESULTS AND ANALYSIS

For comparison of the developed methods, images from variety of sources were used. Many studies examined insect damage in nuts and grains [23] and [24] and that's why insect infected pecan images were chosen for comparison. Oh method was originally developed for text document segmentation, so text document images from [22] and [6] were also selected for comparison. Further, non-destructive images were also taken from [10]. Finally, Reverse Water Flow method was applied to improve pecan defect classification.

4.1 Pecan Images

The selected pecan images consisted of a good pecan (Fig. 7a), a defective pecan with insect exit paths or a pecan with smaller defect (Fig. 7b), and a defective pecan with eaten nutmeat or a pecan with larger defect (Fig. 7c). Twice Otsu method was able to segment the eaten nutmeat (Fig. 7f), but it was unable to segment smaller defects such as insect exit paths (Fig. 7e). Similarly, Jiang method [4] and Kim method [6] were also not successful in segmenting these smaller defects [1]. When the insect exit path orientation (marked 'x' in Fig. 7b) was parallel to the x-ray beam direction then Oh method and Reverse Water Flow method were able to detect the presence of smaller defects: 2 mm diameter insect exit paths. Neither method was able to segment the insect exit path when the orientation was perpendicular (marked 'y' in Fig. 7b). However, the insect exit path marked 'y' in Fig. 7b was segmented by varying the threshold adjustment parameter β (Fig. 8). It is evident that increasing the β resulted in better segmentation of the insect exit paths.
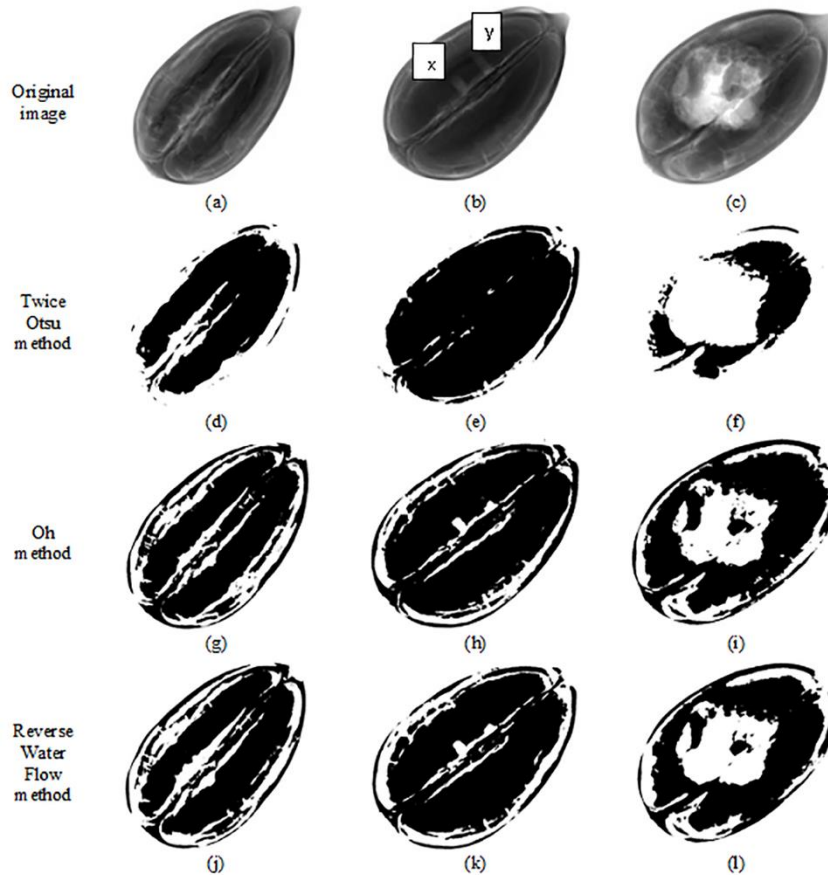
Fig. 7. Segmentation results for pecan images by Oh and Reverse Water Flow methods.

Fig. 8. Effect of threshold adjustment parameter on segmentation results: (a) original image, (b), (c) and (d) segmented image with β = 1.0, 1.5 and 2.0.

4.2   *Text Document Images*

The text document image (Fig. 9a) was taken from [6], and the images in Figs. 9b and 9c were taken from [22]. Segmentation results for the text document images are shown in Fig. 9. Both Oh method and Reverse Water Flow method could segment these images. Smearing of the top line characters in Fig. 9a by Oh method (Fig. 9g) and Reverse Water Flow method (Fig. 9j) may be attributed to deterioration in image quality as the images were taken from on-line journal sources. Reverse Water Flow method produced two good segmentation results out of the three images with same set of parameters, whereas Oh method produced only one good segmentation result.

Fig. 10 demonstrates noise removal by adjusting the threshold adjustment parameter β of Eq. (4) for the text document image of Fig. 9c. It would be pertinent to mention that Oh method required recalculation of optimum thresholds using Eq. (3). The proposed thresholding criterion did not required recalculation of thresholds, but simple adjustment of the lower threshold value by Eq. (4). Savings in computational time by the proposed method over Oh method were not significant for the text images. In these images the widths of characters were small and therefore resulted in shorter travel distances.

Fig. 9. Segmentation results for text document images; original Figs. (a-c), segmented results Kim method (d-f), Oh method (g-i) and Reverse Water Flow method (j-l).
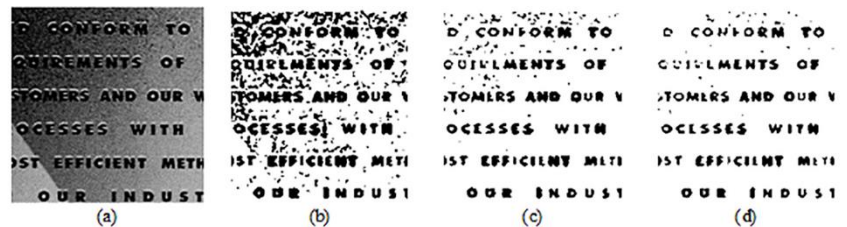

Fig. 10. Segmentation results by Reverse Water Flow method with varying β for noise removal, (a) original image, (b), (c), and (d) segmentation images with β values of 1.0, 2.0, and 2.5.

4.3 *Non Destructive Testing Images*

The Citrus image (Fig. 11a) was taken from [4], and the metal structure image (Fig. 11b) and the cell image (Fig. 11c) were taken from [10]. Both the metal and cell image were segmented successfully by Reverse Water Flow method and Oh method (Fig. 11). However, the citrus image could not segmented properly by the Reverse Water Flow method and Oh method. Poor contrast between background and outer edge of the citrus may be one of the reasons.
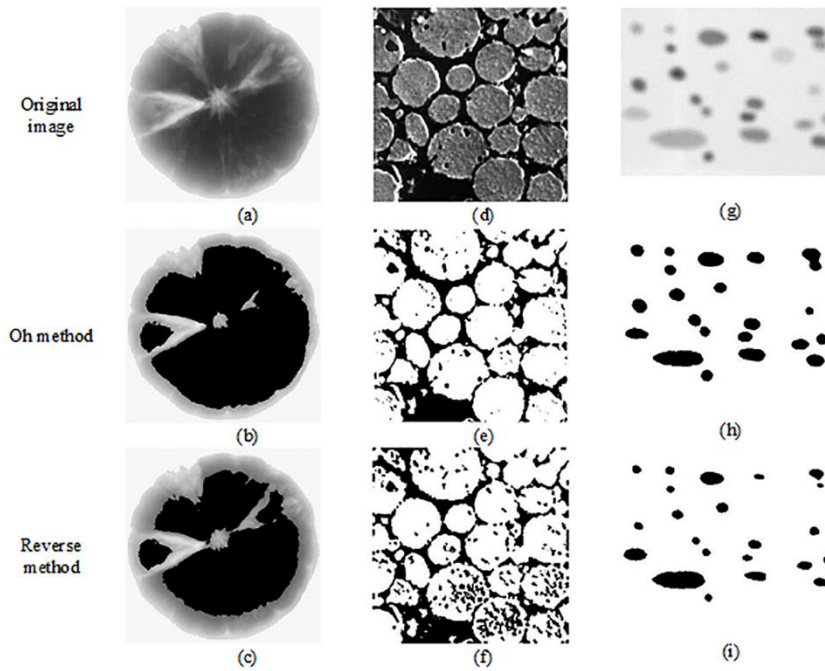
Fig. 11. Segmentation results for citrus image (a), material structure (b) and cell image (c), Oh method (d-f), and Reverse Water Flow method (g-i).

4.4 *Improving Classification Accuracy*

The threshold adjustment parameter (β) was adjusted to maximize classification accuracy [21]. The stopping criterion was assumed as 0.7 to get the water images. The image set consisted of 100 good pecan nuts and 100 defective pecan nuts. The data set was randomly divided into training and testing sets for each classification run. Different β values were input in Eq. 4 to determine the threshold values which were used to segment the resulting water images. Classifiers were trained using the extracted features. Table 1 shows the average of minimum testing error for 20 classification runs. It may be seen that the β values affected classification accuracies.

Table 1 Effect of threshold adjustment parameter β on average minimum testing error of selected classifiers.

Classifier	Average minimum testing error (%) for different β values				
	0.5	2.0	3.5	5.0	7.5
Bayesian	15.95	12.15	12.55	12.70	100.00
Diverse AdaBoost	12.20	8.75	7.50	11.20	10.30
Real AdaBoost	12.45	9.35	7.15	12.15	10.30
Gentle AdaBoost	12.50	9.35	7.15	11.45	10.25

5. CONCLUSIONS

A new local adaptive thresholding method (Reverse Water Flow) and a new multi-level thresholding method (Twice Otsu) were developed for segmentation of unimodal and poor contrast images. The segmentation of the images taken from different sources showed that Reverse Water Flow method was simpler, faster, and more accurate compared to other selected local adaptive thresholding methods. Similarly, Twice Otsu method was a simple multi-level thresholding method suitable for segmentation of larger objects. It is expected that both methods would be able to segment most food and agricultural images. It is also expected that this study would facilitate further development of segmentation methods especially suited for food and agricultural applications.

REFERENCES

[1]   S. K. Mathanker, P.R. Weckler, N. Wang, T. Bowser, N.O. Maness. Local adaptive thresholding of pecan x-ray images: Reverse water flow method. Transactions of the ASABE 53 (3) (2010) 961–969.

[2]   J. Sauvola, M. Pietikainen. Adaptive document image binarization. Pattern Recognition 33 (2000) 225-236.

[3]   Q. Huang, W. Gao, W. Cai. Thresholding technique with adaptive window selection for uneven lighting image. Pattern Recognition Letters 26(6) (2005) 801-808.

[4]   J.E. Jiang, H.Y. Chang, K.H. Wu, C.S. Ouyang, M.M. Yang, E.C. Yang, T.W. Chen, T.T. Lin. An adaptive image segmentation algorithm for x-ray quarantine inspection of selected fruits. Computers and Electronics in Agriculture 60(2) (2008) 190-200.

[5]   C.H. Chou, W.H. Lin, F. Chang. A binarization method with learning-built rules for document images produced by cameras. Pattern Recognition 43(4) (2010) 1518-1530.

[6]   I.K. Kim, D.W. Jung, R.H. Park. Document image binarization based on topographic analysis using a water flow model. Pattern Recognition 35 (2002) 265-277.

[7]   D. Comaniciu, P. Meer. Mean shift: a robust approach toward feature space analysis. IEEE Transactions on Pattern Analysis and Machine Intelligence 24(5) (2002) 603-619.

[8]   M.K. Quweider, J.D. Scargle, B. Jackson. Gray level reduction for segmentation, thresholding and binarisation of images based on optimal partitioning on an image interval. IET Image Processing 1(2) (2007):103-111.

[9]   M.M. Moki, S.A.R.A. Bakar. 2007. Adaptive thresholding based on co-occurrence matrix edge information. Journal of Computers 2(8) (2007) 44-52.

[10] M. Sezgin, B. Sankur. Survey over image thresholding techniques and quantitative performance evaluation. Journal of Electronic Imaging 13(1) (2004) 146-168.

[11] N. Otsu. A threshold selection method from gray level histograms. IEEE Transactions on Systems Man and Cybernetics Part C, Applications and Review 9(1) (1979) 62-66.

[12] S. Arora, J. Acharya, A. Verma, P. K. Panigrahi. Multilevel thresholding for image segmentation through a fast statistical recursive algorithm. Pattern Recognition Letters 29(2) (2008) 119-125.

[13] C.H. Chou, W.H. Lin, F. Chang. A binarization method with learning-built rules for document images produced by cameras. Pattern Recognition 43(4) (2010) 1518-1530.

[14] E.R. Davies. Stable bi-level and multi-level thresholding of images using a new global transformation. IET Computer vision 2(2) 2008: 60-74.

[15] B.N. Saha, N. Ray. Image thresholding by variational minimax optimization. Pattern Recognition 42(5) (2009) 843-856.

[16] D. Sen, S.K. Pal. Histogram thresholding using fuzzy and rough measures of association error. IEEE Transactions on Image Processing, 18(4) (2009) 879-888.

[17] D. Malyszko, J. Stepaniuk. Adaptive multi-level rough entropy evolutionary thresholding. Information Sciences 180(7) (2010) 1138-1158.

[18] E. Cuevas, D. Zaldivar, M.P. Cisneros. A novel multi-threshold segmentation approach based on differential evolution optimization. Expert Systems with Applications 37(7) (2010) 5265-5271.

[19] L.K. Huang, M.J. Wang. Image thresholding by minimizing the measures of fuzziness. Pattern Recognition 28 (1995) 41–51.

[20] S. K. Mathanker. Development of a new local adaptive thresholding method and classification algorithms for X-ray machine vision inspection of pecans. (2010) PhD dissertation, Department of Biosystems and Agricultural Engineering, Oklahoma State University, Stillwater, OK.

[21] S.K. Mathanker, P.R. Weckler, T.J. Bowser, N. Wang, N.O. Maness. AdaBoost classifiers for pecan defect classification. Computers and Electronic in Agriculture 77 (2011) 60-68.

[22] H.H. Oh, K.T. Lim, S.I. Chien. An improved binarization algorithm based on a water flow model for document image with inhomogeneous backgrounds. Pattern Recognition, 38 (2005) 2612-2625.

[23] S.K. Mathanker, P.R. Weckler, T. J. Bowser. X-ray applications in food and agriculture: A review. Transactions of the ASABE (2013) 1227–1239.

[24] S. K. Mathanker, P. R. Weckler, N. Wang. Terahertz (THz) applications in food and agriculture: A review. Transactions of the ASABE (2013) 1213–1226.

Sunil K. Mathanker is with the Department of Agricultural and Biological Engineering, University of Illinois at Urbana-Champaign, Urbana IL USA. His research interests include: development of sensing and control systems to improve efficiency of agricultural machinery, non-destructive testing in food and agriculture sector, and precision agriculture.
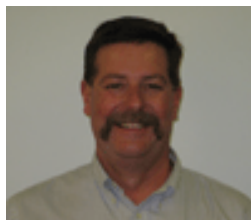
Paul Weckler is with the Department of Biosystems and Agricultural Engineering, Oklahoma State University, Stillwater OK USA. His research interests include: machine vision applications in food and agricultural, and precision agriculture.